Journal of Theoretical Biology 254 (2008) 14–26

Contents lists available at ScienceDirect

Journal of Theoretical Biology

journal homepage: www.elsevier.com/locate/yjtbi

Complex temporal patterns of spontaneous initiation and termination of reentry in a loop of cardiac tissue ☆

H. Sedaghat [a,*], M.A. Wood [b], J.W. Cain [a], C.K. Cheng [c], C.M. Baumgarten [d], D.M. Chan [a]

[a] Department of Mathematics and the Center for the Study of Biological Complexity, Virginia Commonwealth University, Richmond, VA, 23284-2014, USA
[b] Department of Internal Medicine-Cardiology and the Pauley Heart Center, Virginia Commonwealth University, Richmond, VA, 23284-2014, USA
[c] Department of Computer Science and the Center for the Study of Biological Complexity, Virginia Commonwealth University, Richmond, VA, 23284-2014, USA
[d] Department of Physiology and the Pauley Heart Center, Virginia Commonwealth University, Richmond, VA, 23284-2014, USA

ARTICLE INFO

Article history:
Received 31 August 2007
Received in revised form
27 March 2008
Accepted 2 May 2008
Available online 15 May 2008

Keywords:
Loop
Reentry
Pacer
Thresholds
Bistability

ABSTRACT

A two-component model is developed consisting of a discrete loop of cardiac cells that circulates action potentials as well as a pacing mechanism. Physiological properties of cells such as restitutions of refractoriness and of conduction velocity are given via experimentally measured functions. The dynamics of circulating pulses and the pacer's action are regulated by two threshold relations. Patterns of spontaneous initiations and terminations of reentry (SITR) generated by this system are studied through numerical simulations and analytical observations. These patterns can be regular or irregular; causes of irregularities are identified as the threshold bistability (T-bistability) of reentrant circulation and in some cases, also phase-resetting interactions with the pacer.

1. Introduction

Ventricular arrhythmia is the leading cause of cardiac arrest and sudden death. Clinical observations and implantable cardioverter defibrillators (ICD) have accumulated a substantial amount of data on the occurrences of ventricular arrhythmia in patients (Anastasiou-Nana et al., 1988; Lampert et al., 1994; Liebovitch et al., 1999; Lown, 1979; Stein et al., 1992; Wood et al., 1995a, b, 1997). Temporal patterns of initiations and terminations of ventricular arrhythmia tend to exhibit substantial variations across different time scales. Arrhythmia events are not random; they show circadian patterns (Lampert et al., 1994; Wood et al., 1995b) and also tend to occur in clusters. However, the detection times between consecutive events and clusters are spread out over time (Liebovitch et al., 1999; Stein et al., 1992; Wood et al., 1995a) making it difficult to understand their causes and make predictions about their occurrences. Unlike the circadian patterns, these clusterings or their patterns of occurrences are not affected by the long-term administration of antiarrhythmic drugs (Wood et al., 1995a). In spite of the abundant data in existence, the basis for non-circadian patterns is not well-understood.

Many factors, ranging from internal cardiac mechanisms to external chance events play significant roles in shaping the electrocardiogram (ECG) recordings and the implantable defibrillator data. Separating all of the possible contributions is a formidable task, but understanding the influences of various factors and the extent to which each plays a role may have important consequences for the diagnosis and treatment of tachyarrhythmias. In particular, changes in the basic internal cardiac mechanisms might play a significant role in generating and sustaining arrhythmias, especially in diseased hearts.

Recent studies suggest that in at least half of the patients who survive myocardial infarction (MI) the substrate for ventricular tachycardia (VT) is present and substantial evidence exists that VT occurrences in the chronic phase of MI are based on reentry (De Bakker et al., 1990). In a damaged heart, the zone around the dense infarcted scar of dead myocardium is a patchy interwoven matrix of injured and surviving tissue in islands and branching bands (Chow et al., 2002; De Bakker et al., 1990; Downar et al., 1992; Harris et al., 1987). Studies indicate that the surviving tissue has near normal action potential characteristics and reentrant tachycardia may be caused predominantly by the geometric arrangement of surviving fibers (De Bakker et al., 1990). Such geometric arrangements often take the form of loops that can circulate action potentials in a unidirectional fashion, with pulses reentering some of the loops repeatedly. In this case, the circulating action potentials in such loops create reentrant circuits

☆ This research was supported in part by a grant from Medtronic, Inc.
* Corresponding author. Tel.: +1 804 828 5806.
E-mail address: hsedagha@vcu.edu (H. Sedaghat).

0022-5193/$ - see front matter © 2008 Elsevier Ltd. All rights reserved.
doi:10.1016/j.jtbi.2008.05.003

(RC). The rapid oscillation or beat rate of a particular RC may enable it to take over the ventricular contraction cycle and thus generate a VT event.

The relative simplicity of RC and their importance in clinical arrhythmogenesis have made them objects of frequent study (Cain, 2007; Chen et al., 2005; Cytrynbaum and Keener, 2002; Courtemanche et al., 1993, 1996; Courtemanche and Vinet, 2003; Frame and Simson, 1988; Ito and Glass, 1992; Keener, 2002; Mines, 1913; Nagai et al., 2000; Qu et al., 1997; Quan and Rudy, 1990; Sedaghat et al., 2005; Vinet, 2000). Studying spontaneous initiation and termination of reentry (SITR) patterns in the loop context is more focused and simpler than in the whole heart and can offer potentially useful insights into the clinically observed patterns of VT occurrences. Even within the loop context, there are important complications to be aware of. A damaged myocardium is capable of containing several RC which may compete with each other and result is very complicated dynamics. Further, such issues as the geometry of the surviving tissue as well as of the ventricles, the location and size of each loop, the possible interconnections between two or more loops, the manner in which a loop is connected to the healthy parts of the myocardium, as well as tissue heterogeneity and other chemical and physiological aspects of a particular case can each play a role in the creation of complex SITR patterns. But before addressing these various issues, it is necessary to consider an even more basic situation that we believe has not been adequately studied: Can the existence of a *single* loop result in the occurrence of *complex* SITR patterns without appealing to geometric and physiological complexities of the ventricles or to factors external to the heart?

In this paper we answer this question affirmatively despite our own initial skepticism. We use a model that combines a discrete loop with a pacer to form an interactive system. As is commonly done in "restitution-based" models involving loops or fibers, the physiological parameters of the loop are encoded in the restitution functions for action potential duration (APD) and conduction velocity (CV); see e.g. Cain (2007), Cain et al. (2004), Chialvo et al. (1990), Courtemanche et al. (1993, 1996), Courtemanche and Vinet (2003), Fox et al. (2002b), Ito and Glass (1992), Qu et al. (1997), Sedaghat et al. (2005), Stubna et al. (2002) and Vinet (2000). The inclusion of a pacing mechanism is obviously necessary in a study of SITR patterns since reentry needs to be initiated repeatedly if terminations occur. The manner in which the pacer is incorporated into our model is different from previous studies. In our approach the pacer automatically picks up the beat when the circulation ceases in the loop, just as the reentrant circulation automatically overrides the pacer when conditions are right for it. Thus the loop–pacer system in this paper is *self-rebooting* after each mode change to make it possible to record a complete SITR pattern within a single simulation.

In a series of case studies we show that the loop–pacer mechanism may be responsible for irregularities in onset and termination of reentry beyond pervasive physiological and non-physiological complexities. These case studies show that even without such complexities, the SITR patterns generated by our loop–pacer system can be complex; i.e. they contain many regular features yet their evolution over time is difficult to predict. We trace this complexity primarily to the combination of a threshold with bistability of the reentrant circulation. This subtle new feature which we call threshold bistability (T-bistability) is a dynamic realization of basic bistability in the following sense: first, fundamental thresholds are integrated into the model so that they can either trigger reentry or inhibit it. Since basic bistability exists for a range of model parameters, in such cases re-initiations can put the RC in different stable states depending on the *timing* of the re-initiating stimulus from the pacer. In a T-bistable case, at least one of these stable states is a threshold crossing one. In this way, a SITR pattern becomes complex when the crossing of a threshold causes the beat pattern to switch from one stable state to another that crosses a threshold some beats later. Further, it is known that bistability occurs when the length of the loop is within a certain range; see e.g., Sedaghat et al. (2005) and Vinet (2000). Therefore, in our model complex SITR patterns are not seen unless the length of the loop is within that range, with all other physiological parameters in the model held fixed.

2. The threshold model

In this section we describe the main features of the model, leaving a few additional details to Section 4. The pacer is a self-oscillatory mechanism that is tied to the RC (the loop in this paper) via a time lag or delay parameter and a special threshold.

2.1. The loop

Consider a loop of cardiac tissue consisting of cells that conduct action potentials and assume for simplicity that a single conducting pathway connects the loop to the rest of the heart. See Fig. 1, where we assume that the region that is inside the ring and the region that surrounds the ring and its pathway is non-conducting.

Let the physical length of the loop be denoted by L measured in centimeters. Divide the loop into m sets or aggregates of cells, each of which may be called a *cell aggregate* or for brevity, just a "cell." The cell aggregate that is connected to the only pathway out of the loop is also the gateway through which pulses enter the loop or exit it; we label it Cell 1. The assumption that the loop and its pathway are surrounded by non-conducting tissue simplifies the model set up by preventing excitations from entering the loop at any point other than Cell 1. This cell is adjacent not only to Cell 2, but also to Cell m at its other end. For each integer i between 1 and m, label the length of the i-th Cell ΔL_i. These cell aggregates' lengths are not necessarily equal but of course, they add up to L. Since each cell aggregate must have at least one cardiac cell in it, ΔL_i has a natural lower bound, namely the nominal length of a single cardiac cell (about 0.01 cm or 100 μm). The closer all ΔL_i are to this lower bound, the greater is the number m of cell aggregates in a loop of fixed length L. While for discrete modeling it is not necessary to pick m very large, it needs to be large enough (hence each cell aggregate small enough) that the CV from one end of an aggregate to the other can be taken to be approximately constant. This assumption is essential if the restitution of conduction time (CT) is defined in terms of the restitution of CV, as we do later on. It may be of interest to point

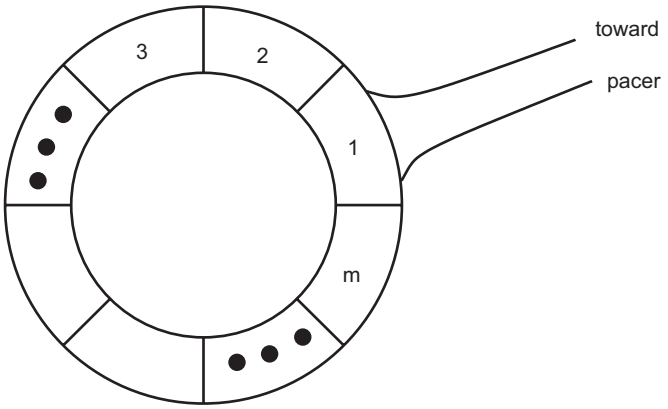

Fig. 1. Schematic diagram of an idealized loop joined to the rest of the heart by a single conducting pathway.

out here that in Chay and Young (1992) five to six cells were found to be necessary for sustaining reentrant circulation in that bifurcation study.

We assume that all the cardiac cells within a given aggregate are identical. If all cells in the *entire loop* have identical physiological characteristics then we may also let cell aggregates all have equal lengths. In such a case, the loop is said to be "homogeneous." Otherwise the loop is "heterogeneous."

To initiate unidirectional circulation, it is necessary that a unidirectional block (UB) exist somewhere in the loop; for simplicity, we place it in Cell 1, the gateway to the loop; see Fig. 1. Thus Cell 1 is able to activate Cell 2, but not Cell *m*. For our simulations, we use a simplified version of the UB time window that is defined by a threshold value for the diastolic interval (DI). Thus conduction is blocked in any cell whose DI is not greater than the threshold DI^*; see Section 4 for more details. Such a minimum value is used in Ito and Glass (1992) as a termination mechanism for explaining the experimental results of Frame and Simson (1988); also see Fox et al. (2002b).

2.2. Restitution functions

We use the term "restitution" generally for relations that give a particular quantity, e.g. APD or CT, as a function of the DI. The DI (usually measured in milliseconds, ms) is the rest or recovery period for the cell which essentially starts with the end of the refractory period and ends when the cell is activated again.

2.2.1. APD restitution

In its most basic form, the APD is the length of time (usually measured in milliseconds, ms) that a cell is active after excitation. For our purposes, we may think of APD as a cell's effective refractory period (ERP) during which no excitations, even strong ones, can elicit new action potentials. The restitution of APD, which can be experimentally measured or derived from ionic models, is the most extensively studied of restitution relations (Banville and Gray, 2002; Cain, 2007; Cain and Schaeffer, 2006; Cain et al., 2004; Cao et al., 1999; Chen et al., 2005; Cherry and Fenton, 2004; Cytrynbaum and Keener, 2002; Gilmour et al., 1999; Hall et al., 1999; Ito and Glass, 1992; Kalb et al., 2004; Koller et al., 1998, 2005; Mitchell and Schaeffer, 2003; Nolasco and Dahlen, 1968; Qu et al., 1997; Sedaghat et al., 2005; Stubna et al., 2002; Ten Tusscher et al., 2006; Vinet, 2000; Watanabe et al., 2001; Watanabe and Koller, 2002). Any APD restitution function, whether experimentally measured or analytically derived can be used in this model. For the numerical simulations in this paper, we use an APD restitution function that is fitted to the experimental data by Koller et al. (2005) where APD values were recorded in two types of patients, those with and those without structural heart disease (SHD). The following is a possible fit to their averaged data displayed in Fig. 1 in Koller et al. (2005) for SHD patients:

$$A(DI) = a_1 - a_2 e^{-\sigma_1 DI} - a_3 e^{-\sigma_2 (DI-\tau_1)} - a_4 e^{-\sigma_3 (DI-\tau_2)^2} + \frac{a_5 (DI-\tau_3)}{(DI-\tau_3)^2 + a_6} \quad (1)$$

with parameter values

a_1	a_2	a_3	a_4	a_5	a_6	σ_1	σ_2	σ_3	τ_1	τ_2	τ_3
350	157	8	20	1700	1200	0.0021	0.025	0.0004	80	136	82

A graph of this function is shown in Fig. 2.

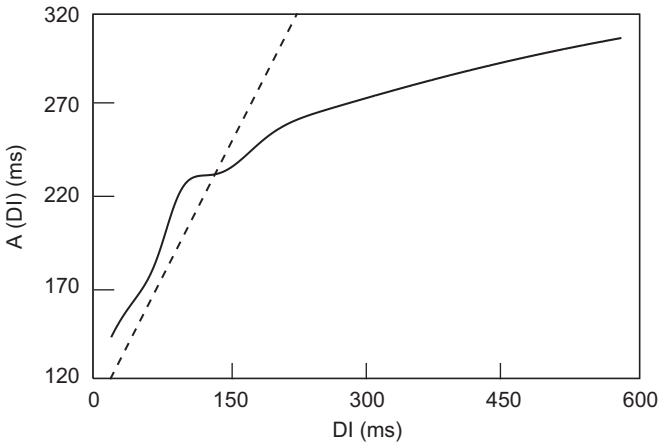

Fig. 2. The APD restitution curve given by Eq. (1). Although not concave, this curve is monotonically increasing. The dashed line has slope 1 and is included for reference.

With regard to using the function (1) as a fit to the experimental data, two points should be stressed: (a) Expressing the APD as a function of DI in the above manner represents only a first order of approximation (see Section 4 below). (b) Since it is usually not possible to determine SITR patterns with quantitative precision (i.e. no single relation exists that gives all possible SITR patterns precisely as a function of parameters) closeness of fit to data is essential only to the extent that variations of slope and concavity over the correct DI ranges in the data are accounted for. These latter variations are important because they affect SITR patterns qualitatively.

2.2.2. CT restitution

Each cell conducts an action potential through it in a finite amount of time. This time interval, usually measured in milliseconds, is referred to as the conduction time (CT) (Cain, 2007; Ito and Glass, 1992; Sedaghat et al., 2005). Experimentally measured CT restitution functions are not as readily available for human hearts as the APD restitution functions; however, they may be readily derived from CV restitution functions through the relation

$$C(DI) = \frac{\Delta L}{V(DI)}, \quad (2)$$

where *C* and *V* are, respectively, the CT and the CV restitution functions. This derivation is valid if as mentioned earlier, *V* is essentially constant over the length of each cell (or cell aggregate) and thus no spatial dependence is required in *V*.

For discussions of CV restitution functions see Banville and Gray (2002), Cao et al. (1999), Chen et al. (2005), Cytrynbaum and Keener (2002), Derksen et al. (2003), Courtemanche et al. (1993, 1996), Courtemanche and Vinet (2003), Frame and Simson (1988), Girouard et al. (1996), Stubna et al. (2002), Ten Tusscher et al. (2006) and Watanabe et al. (2001). For our simulations we use the following expression

$$C(DI) = \frac{\Delta L}{c}[1 + de^{-\omega DI}], \quad DI > 0, \quad (3)$$

with parameter values:

ΔL	c	d	ω
0.1 cm	0.07 cm/ms	1	0.02 ms^{-1}

These numbers are obtained using Eq. (2) and a reasonable fit to the CV data from Girouard et al. (1996) which re-scales guinea

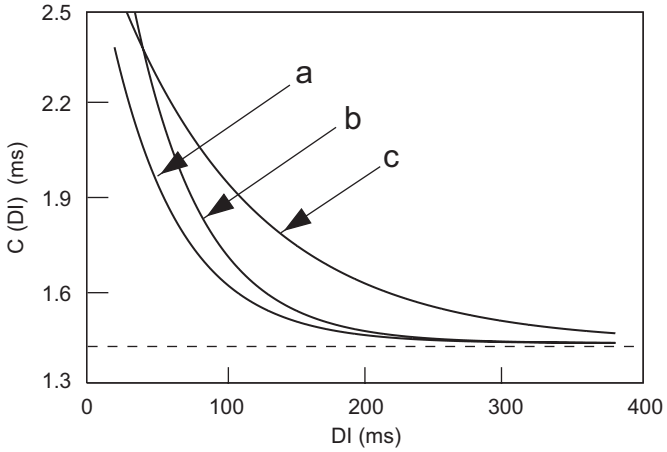

Fig. 3. CT restitution curves given by Eq. (3) for several choices of parameters. For each curve, $\Delta L = 0.1$ and $c = 0.07$. (a) $d = 1$ and $\omega = 0.02$; (b) $d = 1.5$ and $\omega = 0.02$; and (c) $d = 1$ and $\omega = 0.01$.

pig experimental data from Ten Tusscher et al. (2006) by a factor of 0.92 to get the same maximum CV level as in human ventricular tissue. The value of ΔL corresponds to 10 nominal cardiac cells. The number c in Eq. (3) is the maximum CV; in more common (though less uniform) units, the fitted number in the above table would be 0.7 m/s. By changing the parameters in Eq. (3) we may achieve conduction slow-downs in different ways, as shown in Fig. 3.

2.3. The two rhythms

In the absence of reentry, a pacer drives the ventricular contraction cycle. The pacer in this model represents any oscillatory mechanism in the heart other than the RC. It may be taken as the sinus node in which case its primary role is in initiation and re-initiation of reentry if the reentrant circulation fails. At the opposite extreme, it can be an artificial device such as an ICD performing fast, anti-tachycardia pacing in which case the pacer is able to interrupt reentry. If reentry is initiated and interrupted then the pacer and the loop are out of phase and to determine the source of the next excitation, it is necessary to carefully model the alternation between the loop and the pacer. For this purpose we define two rhythms or clocks: the pacer's rhythm which has a prescribed beat pattern (fixed or variable) and the overall loop–pacer system's rhythm which is reset when reentry is initiated or terminated. These two rhythms are related via a pacer threshold (see the next section) and a delay term that we now define.

The *time of occurrence* for the n-th beat (following a fixed reference beat) can be tracked and calculated using the following quantity, namely, the sum of usually variable cycle lengths (after a DI adjustment):

$$\rho_n = \sum_{j=1}^{n} CL_j + (DI_{1,0} - DI_{1,n}), \quad CL_j = A(DI_{1,j-1}) + DI_{1,j}.$$

Next, let the time of occurrence of the k-th *pacer* beat be denoted by β_k (starting from the same reference point in time as that for ρ_n). The difference

$$\beta_k - \beta_{k-1} = B(k)$$

is the duration of each such beat. In our simulations $B(k)$ is defined arbitrarily in order to facilitate our study of the SITR patterns. If the pacer is the sinus node then $B(k)$ is influenced by a variety of deterministic and stochastic factors, such as circadian, weekly and seasonal variations, lifestyles, drugs, the autonomic system and so on. Thus a single, all purpose formula for $B(k)$ does not exist in this case.

The two rhythms ρ_n and β_k are out of phase if reentry occurs as noted earlier. To model their interaction, we define the *first* pacer pulse that reaches Cell 1 in beat n as the *least* integer k_n such that

$$\beta_{k_n} > \rho_n + \delta_n. \tag{4}$$

The index value k_n is generally not easy to find analytically and has to be calculated using a computer program. However, in the simplest case, i.e. when $B(k) = B_0$ is constant (stimuli are equally spaced, each B_0 ms apart) we have $\beta_{k_n} = k_n B_0$ with

$$k_n = \left\lceil \frac{\rho_n + \delta_n}{B_0} \right\rceil,$$

i.e. the least integer that is greater than or equal to the ratio $(\rho_n + \delta_n)/B_0$. The variable delay term δ_n here represents a *time lag* that results from the refractoriness created in the wake of the retrograde wave propagating toward the pacer from the RC. A number of factors may affect the values of δ_n which in general can change from beat to beat. These factors include the different types of tissue in which pulses may propagate (retrograde and antegrade), the electrotonic spread of current in the conducting tissue between the pacer and the loop, and the effect of reentrant waves on the pacer's own intrinsic beat rate, if applicable. These observations suggest that the value of δ_n in general is difficult to model, given the large number of factors that can influence it.

For simplicity we do not consider the electrotonic currents and tissue heterogeneity. Also, if the pacer is not artificial, then we assume that it is protected in the sense that its intrinsic beat rate is not affected by the reentrant activity. In this paper, a simple definition for δ_n such as the following suffices for our qualitative study of SITR patterns:

$$\delta_n = \begin{cases} \delta & \text{if pulse } n-1 \text{ was reentrant} \\ DI^* & \text{otherwise} \end{cases}, \quad \delta > DI^*.$$

The rationale for this definition is as follows: if the loop is not in reentry, then we assume that δ_n takes the minimum value DI^* since Cell 1 must have at least that much rest time after its ERP before it can be reactivated. If the loop is in reentry, then the higher the frequency of reentrant waves, the more persistent is its refractory wake and thus the larger the value of δ. For example, a slow pacer such as the sinus node is typically disassociated by the RC; we model this situation by choosing a sufficiently large value of the delay parameter δ so as to inhibit the pacer from interfering with the reentrant circulation. Small values for δ promote pacer interference in this model; such values may be feasible in certain cases, e.g. if the pacer is an ICD performing anti-tachycardia pacing. During reentry such a device provides bursts of impulses directly into the ventricle that are intended to enter the circuit and terminate reentry.

2.4. Modes and thresholds

We distinguish between two primary dynamic modes for the loop–pacer system: the *reentry mode* where an action potential circulates in the loop by itself and the *paced mode* where the action potential in the loop comes from the pacer. The system's mode in each beat changes on the basis of threshold relations to be defined below. The modes are defined by systems of partial difference equations that track the circulating pulse in both space and time. Introductory material on ordinary and partial difference equations can be found in Cheng (2003), Elaydi (1999), Kocic and Ladas (1993), Mickens (1991) and Sedaghat (2003). Technically, the dynamical system consisting of the loop, the pacer and the associated thresholds is a polymodal structure in the sense of Sedaghat (2003).

2.4.1. Dynamic activation duration

Let $DI_{i,n}$ be the DI of Cell i in beat n. Define the *firing indicator* function as

$$\phi_{1,n} = 1 \quad \text{and}$$

$$\phi_{i,n} = \begin{cases} 1 & \text{if } DI_{i,n-1} > DI^* \text{ and } \phi_{i-1,n} = 1 \\ 0 & \text{if } DI_{i,n-1} \leqslant DI^* \text{ or } \phi_{i-1,n} = 0 \end{cases}, \quad i = 2, \ldots, m.$$

This quantity, which acts as an on–off switch, specifies conditions under which the i-th cell fires an action potential in beat n; these conditions simply require that (a) the preceding Cell $i-1$ fired and (b) the DI of Cell i in the preceding beat $n-1$ exceeded the minimum value DI^* as is required for propagation.

We assume that Cell 1 fires in every beat whether by a reentrant pulse or by a pulse from the pacer.

Let $APD_{i,n}$ denote the APD of Cell i in beat n so that if the i-th cell does not fire in beat n then $APD_{i,n} = 0$ (otherwise, $APD_{i,n} = A_i(DI_{i,n-1})$). The dynamic *activation duration* is defined as the following modified APD

$$\phi_{i,n} A_i(DI_{i,n-1}), \quad i = 1, 2, \ldots, m,$$

where A_i is the APD restitution function for Cell i. Note that $APD_{1,n} = A_1(DI_{1,n-1})$ for Cell 1 in every beat. In the following sections (except in Case study 4) we assume that the loop is APD homogeneous so that $A_i = A$ for all $i = 1, 2, \ldots, m$ where A is given by Eq. (1).

2.4.2. Paced mode

In this mode the pacer determines the DI values $DI_{i,n}$ rather than a reentrant pulse in the primary loop; the circulation is assumed unidirectional owing to an active UB. We use the following system of m equations:

$$DI_{1,n} = \beta_{k_n} - \rho_n \tag{5a}$$

$$\begin{aligned} DI_{i,n} = {} & DI_{i-1,n} + \phi_{i-1,n} A_{i-1}(DI_{i-1,n-1}) \\ & - \phi_{i,n} A_i(DI_{i,n-1}) + C_{i-1}(DI_{i-1,n}) \\ & - C_{i-1}(DI_{i-1,n-1}) + (1 - \phi_{i,n}) DI_{i,n-1} \\ & - (1 - \phi_{i-1,n}) DI_{i-1,n-1}, \quad \text{with } i = 2, \ldots, m. \end{aligned} \tag{5b}$$

Here C_i is the CT restitution function for Cell i. The above system of equations determines the DI values using the first pacer beat after time instance ρ_n (beat n in progress). Fig. 4 illustrates Eqs. (5b) and (6b). The first five terms in Eq. (5b) simply express in mathematical terms what we might state less precisely using the English language. They are the same for tissue fibers as they are for loops; see, e.g. Stubna et al. (2002). The last two terms in the definition of $DI_{i,n}$ in Eq. (5b) allow for proper adjustment of the DI value (without double counting) when Cell i does not fire in beat n (see comments on the reentry mode below). In typical loop models in prior literature all cells fire so these two terms would drop out.

2.4.3. Reentry mode

In this mode the reentrant loop drives the ventricles ectopically. Thus $DI_{1,n}$ is the difference between the APD of Cell 1 and the total CT for unidirectional circulation once around the ring, i.e.

$$DI_{1,n} = \sum_{j=1}^{m} C_j(DI_{j,n-1}) - A_1(DI_{1,n-1}), \tag{6a}$$

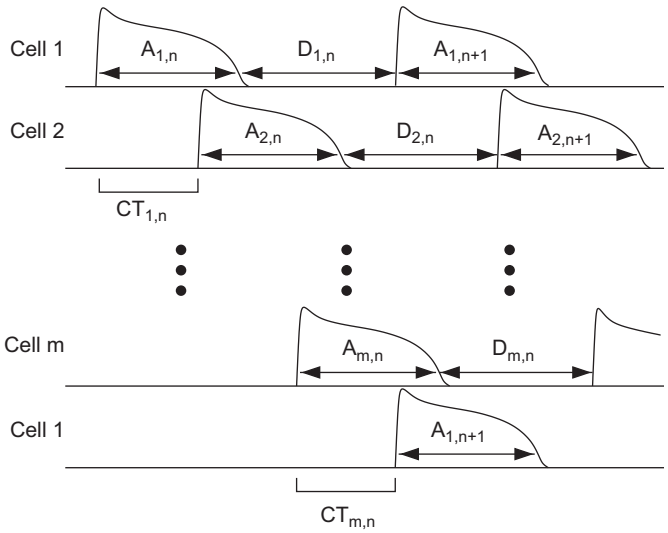

Fig. 4. Schematic diagram of a circulating action potential in a ring of m cells; A is APD, D is DI and CT is the conduction time. The sizes of A, DI and CT are selected arbitrarily for clarity of illustration.

$$\begin{aligned} DI_{i,n} = {} & DI_{i-1,n} + \phi_{i-1,n} A_{i-1}(DI_{i-1,n-1}) \\ & - \phi_{i,n} A_i(DI_{i,n-1}) + C_{i-1}(DI_{i-1,n}) \\ & - C_{i-1}(DI_{i-1,n-1}) + (1 - \phi_{i,n}) DI_{i,n-1} \\ & - (1 - \phi_{i-1,n}) DI_{i-1,n-1}, \quad \text{with } i = 2, \ldots, m. \end{aligned} \tag{6b}$$

It is not hard to show that the system of m equations (6) is equivalent to the coupled map lattice equations in Sedaghat et al. (2005) when $\phi_{i,n} = 1$ for all i and n.

Note that Eq. (6b) is the same as (5b) and the same comments apply. It may be noticed further that when a reentrant pulse is blocked in cell $k < m$ the remaining cells $k+1$ to m in the loop lay dormant until the next excitation. In this case, the last two terms in Eq. (6b) are non-zero to balance the DI values across two adjacent beats (the current, blocked one and the next beat that is initiated by the pacer). These balancing terms are parts of the mathematical formalism needed to distinguish between the two adjacent beats, as are the CT terms appearing in Eq. (6b) for cells $k+1$ to m (recall that each beat is represented in this model by a m-dimensional vector of DI values).

Eqs. (6) are not valid if some of the DI values fall below the threshold DI^* or if a stray pacer pulse gets into the loop (i.e. if the right hand side of Eq. (6a) exceeds the right hand side of Eq. (5a)). The following threshold relations ensure a consistent scenario.

2.4.3.1. Two thresholds. TC: The *circulation threshold* (or *head-tail* or *conduction block threshold*) is based on the following set of inequalities:

$$\sum_{j=1}^{m} C_j(DI_{j,n-1}) - A_1(DI_{1,n-1}) > DI^*,$$

$$\begin{aligned} & DI_{i-1,n} + \phi_{i-1,n} A_{i-1}(DI_{i-1,n-1}) - \phi_{i,n} A_i(DI_{i,n-1}) \\ & \quad + C_{i-1}(DI_{i-1,n}) - C_{i-1}(DI_{i-1,n-1}) > DI^* \quad \text{for } i = 2, \ldots, m. \end{aligned}$$

They ensure that the DI values $DI_{i,n}$ in Eqs. (6) exceed DI^*, as is necessary for the generation of action potentials. If any of the above inequalities fails in a Cell i then a wavefront reaches its own tail in that particular cell and circulation stops until the arrival of the next pacer pulse. In this case we say that TC fails in Cell i.

TP: The *pacer threshold* (or *phase resetting threshold*) is defined by the following inequality:

$$\sum_{j=1}^{m} C_j(DI_{j,n-1}) - A_1(DI_{1,n-1}) < \beta_{k_n} - \rho_n,$$

This inequality ensures that the reentrant pulse (rather than a stray one from the pacer) reactivates Cell 1.

Mode switching criteria: Eqs. (6) are used if TP holds and also TC holds in Cell 1. If for some Cell $i \geqslant 2$ TC fails, then Eq. (6b) can be used to find the DI values for beat n, but we switch to Eqs. (5) for beat $n+1$. If TC fails for $i=1$, or if TP fails then we use Eqs. (5) for beat n.

2.4.4. Bidirectional circulation (BDC) mode

In the absence of UB the pacer sends two pulses in the loop with Cell 1 activating both Cell 2 and Cell m. These pulses propagate in opposite directions to eventually annihilate each other in some cell in the loop. Transitions into and out of this BDC mode are governed by TC, TP and a UB threshold (TUB); see Section 4 below. We assume for simplicity that TUB never fails so that the BDC mode need not be discussed in this paper.

3. SITR patterns

In this section we present the results of numerical simulations of our threshold model along with some analytical observations. Due to the large number of different types of behaviors that can occur by changing one or more of the many variables involved, providing a comprehensive list of essentially different patterns is not feasible here. We therefore present our main results in the form of a few model case studies and for additional results we refer the interested reader to our web site: *www.people.vcu.edu/~hsedagha/SITR*.

Each case study below consists of one or more "runs", i.e. sets of iterations of the propagation equations. Each run is based on a fixed set of parameter values and we call each iteration in a given run a "beat". For each run we need to specify m initial DI values $DI_{i,0}$. This specification of DI values is a technical representation of the occurrence of a premature stimulation in our model.

Computational accuracy is not a major issue in the qualitative studies in this paper. However, calculating the values of the various nonlinear functions (e.g. the exponentials in the APD and CV restitution functions) generate round-off errors that can accumulate in certain cases (e.g. runs in Case study 4). Therefore, results obtained by different programs, codes or levels of precision (single or double) may be different from some of those that we have presented, although the qualitative features are usually retained.

3.1. Mode sequences

The following conventions facilitate the presentation of results in this section:

For a loop consisting of m cells if a reentrant pulse is blocked at Cell j in a particular beat, then we define the *reentry value* of that beat as the ratio $(j-1)/m$; this ratio will be abbreviated as $[j]$.

If a reentrant pulse completes a turn around the loop then the reentry value is 1.

If a reentrant pulse is blocked in Cell j after t complete turns around the loop then the reentry value is $t[j]$.

If a beat occurs in the paced mode (i.e. one of the thresholds TC or TP fails) then we assign it the value -1. Thus t consecutive paced beats appear as $-t$.

If the pattern is locked in the reentry mode, we use the symbol ∞; if it is locked in the paced mode, we use $-\infty$.

Adding up consecutive reentry mode beats and consecutive paced mode beats gives a sequence of numbers consisting of integers whose sign tells us the mode of system in various sets of beats. Examples of mode sequences and more details on them are found in the case studies below.

3.2. Bistability and thresholds

We call the loop–pacer system *bistable* if there are two or more coexisting stable DI configurations or state vectors, each of which can be reached from a particular region of the m-dimensional state space. If there are more than two distinct, coexisting stable states then the system is *multistable*.

A possible cause of bistability (though not the only one) is non-concavity of the APD restitution function (Sedaghat et al., 2005). The APD function (1) whose graph has bumps and twists is also non-concave. Proper CT restitution parameters are required to realize bistability in this case; i.e. the CT and APD restitution parameters must be properly matched. Because the length L of the loop affects the CT through it, bistability may emerge or fade as L is changed with other CT parameters fixed (Sedaghat et al., 2005). For related remarks concerning the occurrence of bistable behavior, see Vinet (2000) where a non-length parameter is used to alter the APD restitution function.

A bistable regime can affect SITR patterns by causing the violation of the circulation threshold TC without any changes in the APD or CT parameters, or any changes in the pacing rate. This situation occurs if the bistable regime satisfies the following *threshold bistability* condition:

T-bistability: There are two distinct stable states in the reentry mode: in one state the DI values cross DI^* and cause the failure of the circulation threshold TC at some cell within the loop, but in the other state the DI values are always greater than DI^*.

An example of T-bistability is shown in Fig. 7; other examples of T-bistability occur in the next section (Case study 1). The m-dimensional state space of a T-bistable system is partitioned into two regions or basins of attraction. As an SITR pattern evolves with the motion of the DI state vector, mode changes occur if the state vector crosses over into the basin of attraction of a different stable regime.

3.3. Case study 1: T-bistable reentry

In this section we establish that T-bistability lends a measure of unpredictability to SITR patterns that is not due to phase resetting disruptions by the pacer (i.e. TP failures). For instance, comparing the mode sequences in Runs 1.2, 1.4 and 1.6 below we see that the initial few bursts of fast, reentrant beats provide no obvious clues about the eventual modes that the patterns lock into.

Consider a homogeneous loop with the APD and CT restitutions given by Eqs. (1) and (3). We also set the length L and other parameters as

L	m	DI^*	δ	B_0
12.5 cm	125	15.3 ms	120 ms	320 ms

where B_0 is the fixed cycle length of the pacer; it is chosen small in this case study to facilitate re-initiations of reentry. The value of δ is set high enough to inhibit pacer interference (TP never fails) as

is typically the case. The following table summarizes the results of simulations; it is followed by a series of observations and elaborations.

Run no.	$DI_{i,0},\ i=1,\ldots,125$ (ms)	SITR pattern mode sequence
1.1	200	$\{-2,2,-2,2,\ldots\}$
1.2	100	$\{-2,4,-2,32[73],-2,\infty\}$
1.3	80	$\{-1,\infty\}$
1.4	70	$\{4,-2,14,-2,4,-2,22[49],-\infty\}$
1.5	60	$\{\infty\}$
1.6	50	$\{11,-2,4,-2,27[57],-2,\infty\}$

(i) In Run 1.1 the SITR pattern immediately locks into a regular form of 2 paced beats followed by 2 reentrant beats. In Runs 1.2, 1.3, 1.5 and 1.6 the SITR pattern locks into the reentry mode. In Run 1.4 the paced mode is locked into. Note that the only thing that is changing from one run to the next is the initial DI values.

(ii) In Runs 1.2, 1.3, 1.5 and 1.6 the DI values in the sustained or locked reentry modes converge to a fixed number and the eventual values of the fundamental parameters are

DI	APD	Cycle length $CL=APD+DI$
59.4 ms	173.6 ms	233 ms

The fixed, limiting DI value 59.4 represents a stable *convergent state*. This equilibrium DI is locally stable (attracting) because using the restitution functions (1) and (3) we compute (Cain, 2007; Ito and Glass, 1992)

$$A'(59.4)+C'(59.4)=0.90<1.$$

(iii) In Runs 1.2, 1.4 and 1.6 all the spontaneously terminated reentry bursts have oscillating (quasiperiodic) DI. Thus APD and CL also oscillate similarly. The oscillatory state is stable and eventually crosses $DI^*=15.3$ ms. Hence there is T-bistability (the oscillatory one and the convergent one) which is responsible for mode changes in each run.

For example, in Run 1.2 the second initiation of reentry (the 32-beat burst) starts with the DI state vector in the basin of attraction of an oscillatory state which expands enough for the DI values to cross DI^* (TC fails); see Fig. 5. This terminates the second reentry burst at Cell 73 in the 41st beat. This is the same type of termination mechanism as that in Fox et al. (2002b), Frame and Simson (1988) and Ito and Glass (1992); this type of oscillations in DI are also seen in Watanabe et al. (2001) where they are related to T wave alternans in ECG recordings; also see Kunysz et al. (1997) in this regard. With the third initiation of reentry, the DI state vector falls in the basin of attraction of the convergent state which then effectively "traps" the DI trajectory and locks the SITR pattern into the reentry mode (here then, simplicity of behavior is not a good thing).

(iv) Examination of the simulation data for Run 1.4 shows a recurrent failing of TC in Cell 1 after the last burst of 23 reentrant beats. For all sufficiently large values of n,

$DI_{1,n}$	$APD_{1,n}$	CL_n
96.6	223.4	320

The number 96.6 is the equilibrium DI for the paced mode with pacing period $B_0=320$. The paced-mode equilibrium happens to be stable because in the absence of reentry the paced mode is governed by the one-dimensional difference equation

$$DI_{1,n}=F(DI_{1,n-1})=B_0-A(DI_{1,n-1}),$$

with $F'(96.6)=-A'(96.6)=-0.901$; i.e. $|F'(96.6)|<1$. Why the transition to the stable paced equilibrium occurs in this run and not others is unclear. Fig. 6 shows the changes in DI values in this run.

(v) In Run 1.5, the given initial DI values put the state vector in the basin of attraction of the convergent state of the system. This is evidently not the case in Run 1.6 with even shorter DI. In Run 1.6, as in Run 1.4, the initial mode is oscillating-DI reentry.

3.4. Case study 2: non-T-bistable reentry

We now consider some longer loops than in Case study 1 for comparison. In these loops bistability is present but does not satisfy the T-bistability condition. A smaller variety of different SITR patterns are obtained (with all other system parameters having the same values as in Case study 1). We consider two different lengths:

$L=13$ cm ($m=130$) where stable oscillating states exist all of which fail TC, but the convergent mode is absent since the DI fixed point of about 62.5 ms is unstable (Cain, 2007; Ito and Glass, 1992)

$$A'(62.5)+C'(62.5)=1.013>1.$$

$L=14$ cm ($m=140$) where all of the stable oscillating states (there is at least one) satisfy TC. The convergent mode is again absent for the same reason as above:

$$A'(68)+C'(68)=1.253>1.$$

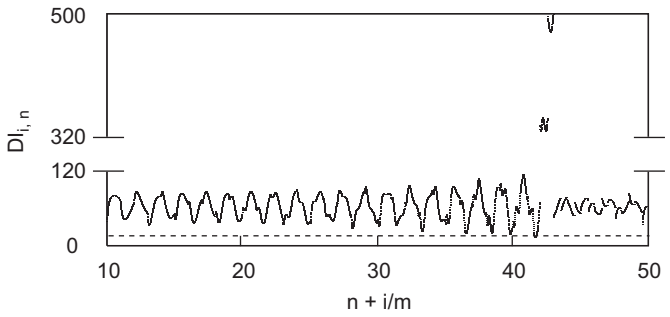

Fig. 5. Results of Run 1.2, showing variation of DI in Beats 10–50. The dashed line corresponds to $DI^*=15.3$. Amplification of oscillations in DI leads to termination of reentry in Beat 41, Cell 73 because $DI_{73,41}<DI^*$. With Beat 44 reentry is re-initiated and the system locks into the stable convergent state (after some transient oscillations).

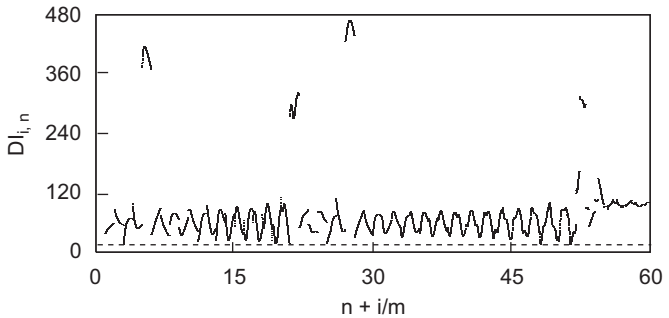

Fig. 6. Results of Run 1.4, showing variation of DI in Beats 1–60. The dashed line corresponds to $DI^*=15.3$. The four interruptions of reentry due to conduction block (TC fails) are seen as brief jumps to high DI. The last interruption terminates reentry and locks the system in the paced mode.

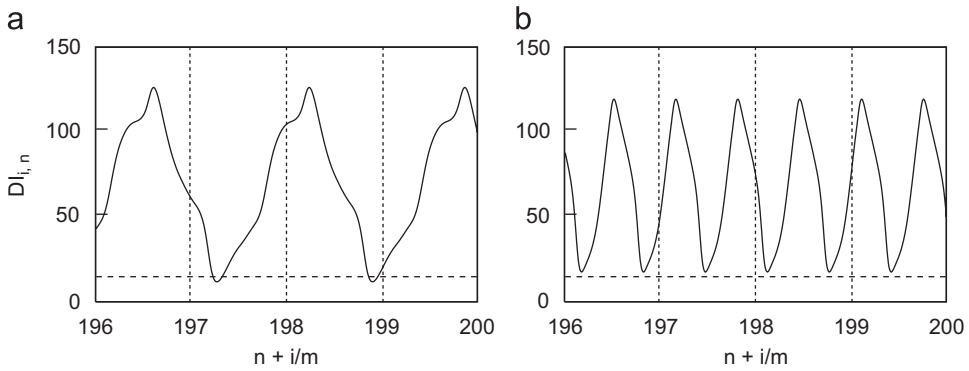

Fig. 7. Two distinct stable states illustrating T-bistability in Run 3.1. (a) If $DI_{i,0} = 67$ for all i, the graph crosses the dashed horizontal line $DI = 15.3$; for the sake of illustrating the quasiperiodic nature of oscillations in reentry mode, the graph ignores TC since reentry would terminate with the first such crossing. (b) $DI_{i,0} = 66$ for all i. Reentry is sustained and the variation of DI is quasiperiodic.

To save space let us abbreviate repetitions or locked mode patterns with bars:

$$\overline{k, -j} = k, -j, k, -j, \ldots \ . \tag{7}$$

The following table summarizes the results of simulations; it is followed by a series of observations and elaborations.

Run no.	$DI_{i,0}$ (ms)	$L = 13$ cm	$L = 14$ cm
2.1	200	$\{\overline{-2, 2}\}$	$\{-2, 2, -2, \infty\}$
2.2	100	$\{-2, 4, -2, 12[60], \overline{-2, 2}\}$	$\{-2, \infty\}$
2.3	80	$\{\overline{2, -2}\}$	$\{-1, 1, -2, 2, -2, \infty\}$
2.4	70	$\{12, -2, 10[79], -2, 17[79], \overline{-2, 5[79]}\}$	$\{12, -2, 2, -2, \infty\}$
2.5	60	$\{56, \overline{-2, 2}\}$	$\{-1, 10, -2, 9, -2, \infty\}$
2.6	50	$\{3, -2, 4, -2, 12[60], \overline{-2, 2}\}$	$\{-\infty\}$

(i) The SITR patterns for the 14 cm loop are expected to lock into the reentry mode since the stable states do not fail TC to cause terminations. The exception is Run 2.6 where possibly owing to the greater length of the loop, a pulse from the pacer has time to activate Cell 1 and block the premature simulation from reentering the loop (threshold TP fails). It is not clear why reentry does not re-initiate as in Run 2.5.

(ii) In the case of the 13 cm loop the repeated terminations can be attributed to the fact that the stable states all fail TC; thus the patterns cannot lock into the reentry mode.

(iii) For both of these loops, the eventual form of the SITR pattern is more predictable than the T-bistable loop of Case study 1. On the other hand, the transient bursts of fast beats still seem difficult to predict.

3.5. Case study 3: special patterns

Run 3.1 (*More T-bistability*). This run presents a complex SITR pattern that locks into a long cycle of several initiations and terminations. Make the following changes to parameters in Run 1.2:

d	B_0
1.3	315 ms

Note that the increase in d from 1 to 1.3 in this run causes a slight elevation of the CT restitution curve (i.e. a conduction slow-down) at low DI values; see Fig. 3.

(i) In this run, after a transient period of spontaneous initiations and terminations, a long 62-beat pattern emerges that is repeated; i.e. the SITR pattern locks into a 62-beat cycle containing several bursts of fast reentrant beats. The mode sequence for this run is as follows, with the pattern between starred numbers repeating:

$$\{-2, 8[81], -1, [35], -2, 4, -2, 7[24], -1, [18],$$
$$-2, 8[18],^{*} -1, [12], -2, 7[12], -1, [12], -2,$$
$$10[49], -2, 5[49], -2, 4, -2, 7[22], -1, [19],$$
$$-2, 7[19],^{*} -1, [12], -2, 7[12], -1, [12], -2, \ldots\}.$$

(ii) The DI equilibrium of approximately 64 ms is unstable in this run since

$$A'(64) + C'(64) = 1.073 > 1.$$

This instability is caused by the greater value of d and results in the absence of the convergent state. Nevertheless, there is T-bistability where one of the stable oscillating states does not fail TC but another oscillating state does. In the first oscillatory state, DI values come very close to DI^{*}; see Fig. 7. This proximity increases the sensitivity to transient effects of mode changes and makes locking into the reentry mode an improbable event.

Run 3.2 (*Pacer action*). In Case studies 1 and 2 we see that the convergent reentry pattern is " sticky", i.e. once this pattern is attained, reentry does not self-terminate by the circulation mechanism in the loop. However, if the pacer is able to get a pulse into the loop (see Section 2.3) then it can cause termination of reentry by changing the convergent pattern to a terminating oscillatory one in a T-bistable case. This run illustrates this situation.

All parameters are as in Run 1.5 (hence there is T-bistability) except that now:

δ	B_0
45 ms	800 ms

We have set the pacing period at the nominal sinus length to eliminate the effects of fast pacing. The smaller value of δ promotes interference by the pacer.

(i) The mode sequence for this run, which may be compared with Run 1.5, is

$$\{40, -1, 15, -\infty\}.$$

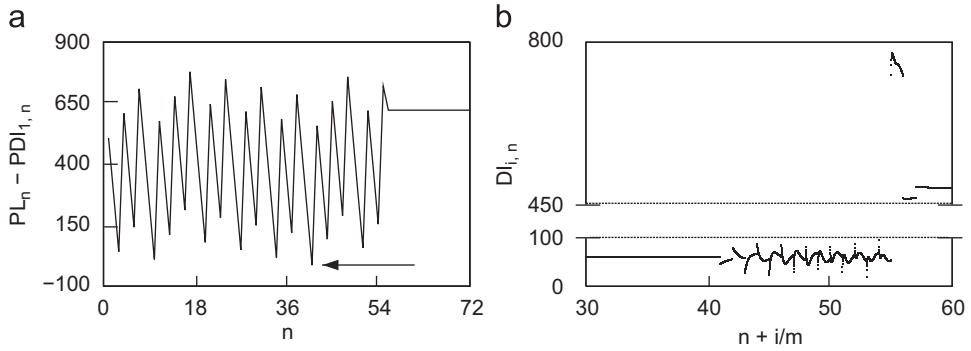

Fig. 8. Results of Run 3.2. (a) Variations in $PL_n - PDI_{1,n}$ (see text). The negative value in Beat 41 (indicated by the arrow) corresponds to termination of reentry due to failure of TP. (b) DI values in Beats 30–60; note the phase resetting that occurs in Beat 41 and changes the reentrant circulation pattern from convergent to oscillatory in this T-bistable case.

(ii) Reentry is initiated with Beat 1 by a premature stimulation, and the DI values begin to approach the limiting value 59.4 ms as in Run 1.5. However, TP fails in Beat 41; a stray pulse from the pacer enters the loop and changes the reentry DI pattern from the convergent type to an oscillating one; see Fig. 8. The quantities PL_n, $PDI_{1,n}$ in Fig. 8 are the right hand sides of Eqs. (5a) and (6a), respectively.

The oscillating DI pattern crosses the DI^* threshold (TC fails) in Beat 55 and reentry terminates in this beat.

3.6. Case study 4: slow pacing, heterogeneity and PVCs

When the pacing period is long (say, within the nominal sinus range of 800 ± 350 ms) and the loop is homogeneous, *re-initiations* of reentry do not occur with the above CT and APD parameters in the absence of premature stimulations or ectopic sources. The low CT (or high CV) in the loop blocks reentry when pacing is slow. Nevertheless, the rather common occurrences of VT at low pacing rates in patients (Winkle et al., 1977) motivate us to study this important special case in the context of a heterogeneous loop with a variable-rate pacer.

Suppose that the loop consists of two patches of cells. Patch 1 consists of cells 1 through j and Patch 2 contains cells $j+1$ and beyond where of course, j is a positive integer less than m, the total number of cells. The cells in Patch 1 may have different APD and/or CT restitution parameters than those in Patch 2. For simulations, we also assume that the pacer has a variable-rate within the aforementioned nominal sinus range. Assume that the pacer's oscillation period varies in a sinusoidal fashion:

$$B(k) = B_0 + B_1 \cos\left(\frac{2\pi k}{w}\right).$$

This beat pattern may represent an idealization (without random effects) of a single cycle of a complex, multi-pattern stretch of pacer beats. More complex variations may be considered in later studies if needed.

The number w is the period of a full cycle of variable-rate oscillations, which we refer to as a *full pacing cycle* (FPC). The halfway point of the FPC, or the "bottom of the FPC well" occurs at $k = w/2$; at this point, the pacer oscillates with minimum period (fastest beat rate). On the other hand, when $k = 0$ or $k = w$ the pacer has its largest oscillation period (slowest beat rate). The number B_1 is the FPC "amplitude" since it modulates the pacer's oscillation period within the FPC. If $B_1 = 0$ then the period is a fixed B_0 as in the preceding case studies.

Run 4.1. We fix the APD and CT parameters for Patch 2 to be the same as those used in Case study 1. Patch 1 APD and CT have the same parameters as Patch 2 except for the following:

a_1	a_2	c
300 ms	170 ms	0.05 cm/ms

Thus APD is reduced (by a shift in the restitution function) in Patch 1; also the cells in this patch conduct more slowly with a lower value of c (the maximum CV). Additional loop and pacer parameters are set as follows:

L	B_0	B_1	w	j	δ	$DI_{i,0},\ 1 \leqslant i \leqslant 135$
13.5 cm	800 ms	350 ms	1000	50	140 ms	600 ms

The integer j gives the number of cells in Patch 1 and the three pacing parameters w, B_0 and B_1 define a variable pacing protocol with FPC period of 1000 beats and amplitude 350 about a fixed, nominal sinus trend of 800 ms.

(i) The mode sequence of the SITR pattern obtained is

$$\{-464, [51], -1, [51], -1, [51], -1, [51], -1, [51], -2, \infty\}.$$

(ii) The mode sequence exhibits a pattern of five incomplete reentry initiations followed by a pacer beat (or two in one case). Each incomplete reentry start which is blocked at the patch junction (Cell 51) corresponds to a short cycle length (about 224 ms) compared to the pacer's period of approximately 460 ms near the middle of the FPC. Hence the pattern of five alternating reentry/pacer beats resembles a series of premature ventricular contractions (PVC) in a bigeminal form before reentry finally takes hold for good.

(iii) We note that if $j = 40$ or fewer, then no reentry is initiated in this run. On the other hand, larger j than 50 sustain reentry more quickly by increasing the percentage of slow cells in the loop.

Run 4.2. In the preceding run the pacer did not interfere with the reentrant circulation (TP did not fail) because $\delta = 140$ ms was large enough to block the pacer. We now show that decreasing δ to promote pacer interactions may cause the eventual termination of reentry in the preceding run. We make only one change in this run relative to Run 4.1 by setting $\delta = 70$ ms.

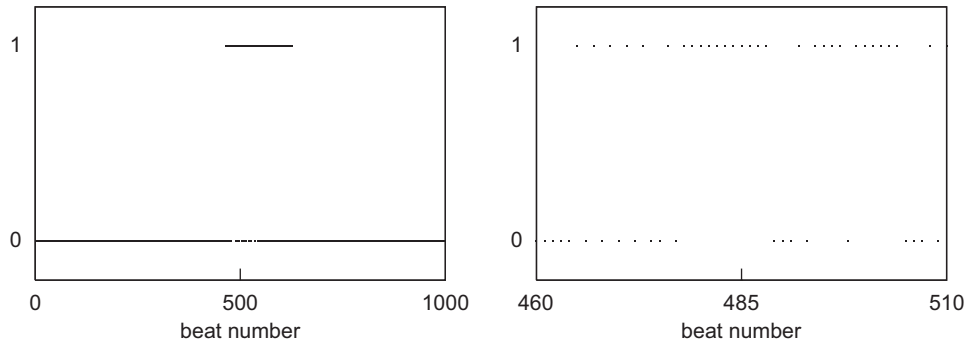

Fig. 9. Schematic diagram of mode changes in Run 4.2. Beats in the reentry mode are listed with value 1 and those in the paced mode are given the value 0.

(i) The mode sequence of the resulting SITR pattern is as follows:

$$\{-464,\underbrace{[51],-1,\ldots,[51],-1}_{4\ \text{times}},[51],-2,1,-1,11,$$
$$-3,1,-1,4,-1,6,-3,1,-1,4,-1,6,-3,1,-1,11,-1,6,$$
$$-3,\underbrace{[51],-1,\ldots,[51],-1}_{38\ \text{times}},[51],-374,\ldots\}.$$

After several PVCs and reentrant bursts of different durations, the pattern locks into the paced mode until reentry is initiated in the next FPC. This mode sequence is sensitive to computer round-off errors; however, the varied nature of mode changes persists. Fig. 9 gives a graphical representation of mode changes for this run.

(ii) The first deviation from the mode sequence of Run 4.1 occurs with a TP failure that interrupts reentry after just one full cycle. Some of the −1 entries in the mode sequence above (mostly the ones *not* associated with conduction blocks in Cell 51) indicate failures of TP also.

4. Further details of the model

In this section we present additional supporting details about the model.

4.1. Remarks concerning the APD restitution function

4.1.1. Memory and latency

Experimental measurements and other studies reveal the difficulty of fitting a single curve to the data, particularly at the lower end of the DI scale. To address this and related issues, refinements have been considered in the forms of memory and latency. Beat to beat memory has been studied in Chialvo et al. (1990), Fox et al. (2002a); Gilmour et al. (1999), Glass et al. (1987), Jalife et al. (1982), Otani and Gilmour (1997), Watanabe et al. (2001) and has been modeled in a number of ways. In many cases, modeling memory can be accomplished by using DI values from several earlier stimulations. Latency (roughly a brief period between the arrival of a pulse and the firing of the cell) has also been expressed as a restitution function of DI (Derksen et al., 2003; Chialvo et al., 1990). If this effect is added to APD we obtain a composite restitution function that may no longer be monotonic for small DI values. For simplicity, we ignore both memory and latency in this paper; however, they can (and need to) be included in the model for greater refinement in future studies.

4.1.2. Standard vs. dynamic protocols

The APD restitution function may be measured experimentally using two different pacing protocols: dynamic or standard (S1–S2) (Kalb et al., 2004; Koller et al., 1998). These protocols generally produce APD curves that are shifted or have different slopes. For a discussion of this issue regarding the APD restitution that we use in this paper see Koller et al. (2005). The fit in Eq. (1) is to the dynamic restitution data in Koller et al. (2005).

4.1.3. Remodeling

The APD values (and thus the restitution function) may be affected by the steady fast pacing of the ventricles (Krebs et al., 1998) or of the atria (Manios et al., 2005). The implied shift in the APD restitution can have a significant effect on the SITR patterns in certain borderline cases. For simplicity we do not consider such effects in this paper; however, a suitable modification of the APD restitution function that incorporates explicit time dependence can accommodate dynamically induced shifts.

4.1.4. APD non-monotonicity and spatio-temporal chaos

Experimental evidence is offered in Stubna et al. (2002) that the APD restitution curve may be non-monotonic for small DI values. Working with an APD restitution curve having a single local minimum at low DI, the same study demonstrates the occurrence of spatial bifurcations along the length of a periodically paced fiber of cardiac tissue. Although not involving a loop structure, the work in Stubna et al. (2002) uses restitution functions in a discrete model. A localized form of non-monotonicity (like a bump or dent) in APD may occur at any DI value and has interesting consequences for additional complexity in reentry mode. In Qu et al. (1997) where a continuous model of the loop as a cable is used, this type of non-monotonicity is shown to be responsible for the appearance of spatio-temporal chaos in APD and other key variables over the length of the loop. The occurrence of spatio-temporal chaos on the loop may raise the level of unpredictability in SITR if the amplitudes of oscillations in DI are large enough to let the wavefront reach its tail (thus causing a threshold failure).

4.2. Restitutions of ionic currents and conduction block

Various anatomical and functional mechanisms for UB in a loop are discussed in the model study (Quan and Rudy, 1990). These mechanisms include a properly timed premature stimulus delivered to a suitable location in the loop, inhomogeneities in the degree of cellular uncoupling and gap junction resistance, in membrane excitability and in fiber cross sectional area. The discussion in Quan and Rudy (1990) points to time, space and voltage "windows of vulnerability" for the occurrence of UB and initiation of reentry. Of these, the time window is seen to be the

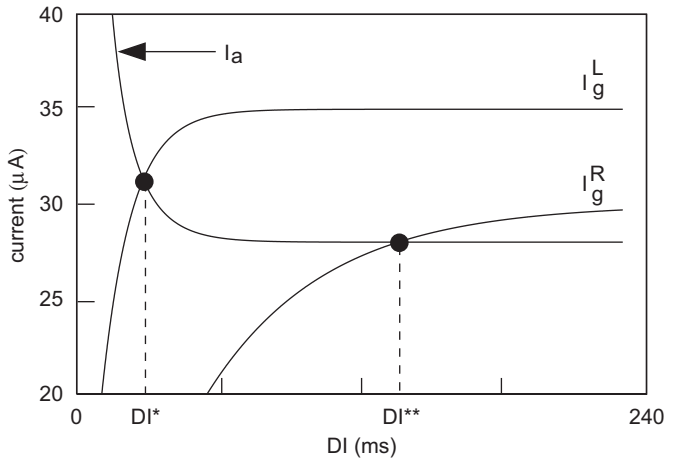

Fig. 10. Activation and generated currents restitution curves illustrating the definition of DI^* and DI^{**}. In this figure, $I_a = I_a^L = I_a^R$ (see text).

easiest to measure and its value is related to the space and voltage windows via standard mathematical formulas.

Each cell requires a certain amount of depolarizing current to fire an action potential. This *activation threshold* can be represented by a restitution function (Jack et al., 1975) or equivalently, the strength–interval curve (Chialvo et al., 1990) shifted to the left so that the origin represents the end of the ERP. In Fig. 10 this curve is shown as a decreasing restitution function I_a.

In principle, at any time following the end of the ERP a sufficiently large current will be able to elicit an action potential. However, in the absence of external electrical shocks, there is a limited amount of current I_g available to depolarize the next cell. If a restitution of I_g is given then the intersection point of I_a and I_g is the DI threshold or cut-off value DI^* in the sense that if $DI > DI^*$ then action potential is fired and propagation occurs. The time interval DI^* is similar in nature to the chronaxie (Plonsey and Barr, 2000) although the definition of DI^* requires another restitution curve in addition to I_a. A monotonically increasing restitution function for I_g might be appropriate; see Fig. 10.

For our purposes here we do not need explicit formulas for either I_a or I_g. The value DI^* may be chosen arbitrarily or estimated experimentally without reference to its potential sources. Values as high as 160 ms were used in Ito and Glass (1992). In human cases the value of DI^* in vivo is likely to be in a much smaller range. We use the conservatively small value of about 15 ms in this study.

An analog of the time window in Quan and Rudy (1990) can be defined here using the restitution functions I_a and I_g. We define two sets of currents restitution functions for Cell 1 corresponding to the two possible directions in the loop: I_a^L, I_a^R and I_g^L, I_g^R for the "left" and the "right" directions. The asymmetry creates a *UB window* in Cell 1 as follows: Let $I_a^R \geqslant I_a^L$ and $I_g^R \leqslant I_g^L$ with at least one of these inequalities strict. Let DI^* be the (unique) intersection point of I_a^L and I_g^L and let DI^{**} to be the intersection point of I_a^R and I_g^R. Then $DI^* < DI^{**}$ and the interval between these two values is where the UB occurs. For if $DI_{1,n}$ represents the DI of Cell 1 in a cycle or beat n, then the conditions

$$DI^* < DI_{1,n} < DI^{**}$$

imply that propagation is possible in one direction because the threshold marked by DI^* is crossed but it is inhibited in the other direction where the DI^{**} threshold is not crossed.

We emphasize that the UB as defined here is functional and may not occur even if the UB window exists (for anatomical or functional reasons). If the number $DI_{1,n}$ does not enter the UB window (i.e. the interval from DI^* to DI^{**}) in a particular beat n then the UB does not materialize. This option adds another mode to the loop–pacer system, namely the BDC mode mentioned previously. In addition to TC and TP, the following threshold is associated with the BDC mode:

TUB : $DI_{1,n-1} < DI^{**}$ with beat $n-1$ in the paced mode.

This inequality defines the *UB threshold* to ensure that Cell 1 conducts unidirectionally. If beat $n-1$ is in reentry mode then conduction in beat n is automatically unidirectional whether TUB holds or not, because the pulse is transmitted from a still active Cell m. To limit the variety of cases to consider, we assume in this paper that DI^{**} is so large that the UB is always present in Cell 1 (permanent UB), so TUB always holds.

5. Discussion and summary

In the preceding sections, we developed a loop–pacer threshold model to investigate occurrences of complex SITR patterns under minimally complicated physiological conditions. Our study involves a new construct in loop modeling, namely a combination of the loop and the pacer as a single dynamical system that is capable of switching between reentrant and paced modes automatically as one threshold or another is crossed. While the model's basic ingredients are well known in the literature that we have cited in this paper, to our knowledge the particular loop–pacer approach that we have taken here is new. Using experimental data on APD and CV restitution parameters for ventricular tissue in SHD patients we obtained various conditions and parameter values that yielded irregular SITR patterns. Since VT events in hearts with MI are often generated by RCs, our finding suggests that deterministic internal cardiac mechanisms may contribute to irregular occurrences of VT events along with other factors that are external to the heart, whether or not they are deterministic in nature.

The model also has significant limitations in the context of human hearts. It is designed for studying the occurrences of complex SITR patterns in a single-loop scenario in a precise and conclusive fashion. However, the model is not designed to comprehensively explain VT occurrences in a real heart. It does not include all relevant geometric and physiological parameters that may shape the evolution of an SITR pattern along a different, presumably even less predictable course than the one we have considered. The model's response to factors external to the heart (e.g. circadian changes, variations in autonomic tone, effects of drugs, stress, exertion, deteriorations in tissue caused by damage, etc.) is restricted to changes in APD and CT restitution functions and the pacer's beat pattern.

We found that a major cause of unpredictable behavior in the model is T-bistability where at least one stable regime causes a failure of the circulation threshold TC. In this situation the initiation and termination of reentry depend on the position of the DI state vector in the m-dimensional state space immediately prior to re-initiation of reentry. Since nonlinearity in propagation equations makes it difficult to track the state vector, it is difficult to forecast the long-term behavior of an evolving SITR pattern for a T-bistable loop.

Bistability of a different type, akin to our two *modes* rather than to the dynamic states that define T-bistability (or basic bistability in Sedaghat et al., 2005; Vinet, 2000) was demonstrated in Chay and Young (1992) in computer-generated bifurcation diagrams. A six-cell loop model was used in Chay and Young (1992) which uses the ionic Beeler–Reuter model (rather than restitution relations) to define the physiological parameters. The work in Chay and Young (1992), which does not deal with SITR patterns, showed the

coexistence of three states (or modes)—reentrant circulation, ectopic self-beating and quiescent—all of which can be triggered by electrical impulses given at the precise time and magnitude.

The abstract nature of our model makes it applicable in a number of different settings. It should be clear from the model's set up that the APD, CT and other physiological parameters of the loop need not come from human ventricular tissue, but can come from any experimental or hypothetical setting. The pacer, as we have already remarked, can be natural or artificial. A number of prior studies of a different nature from ours also discover complex SITR patterns in simple settings, such as in sheets (Bub et al., 2003; Hwang et al., 2005), loops (Nagai et al., 2000) and aggregates (Kunysz et al., 1997) of animal cardiac tissue. In Bub et al. (2003) and Hwang et al. (2005) complex patterns in monolayers of growing cell cultures are linked to changing densities and to local inhomogeneities, respectively. In Kunysz et al. (1997) bursting beat patterns are studied in cell aggregates under external pacing. Closer to the subject matter of this paper, in Nagai et al. (2000) a ring-shaped lab preparation is considered with two localized pacemakers. Threshold relations for handling the pacers in this loop appear in the mathematical discussion. In our model the pacemaker is not within the loop; a non-trivial modification of our mathematical set up would be required to allow bidirectional propagation and account for the annihilation of opposing pulses.

In a different class of studies, namely, the "modulated parasystole," a permanent ectopic rhythm (rather than RC) coexists with the sinus or another competing rhythm. In such relatively simple systems, complex beat patterns arise that are highly sensitive to parameter changes (Glass et al., 1987; Jalife et al., 1982; Moe et al., 1977). Like the TP threshold in our model, a mathematical relation with a discontinuity is responsible for the complexity of temporal patterns in parasystole; see Glass et al. (1987), Moe et al. (1977).

We omitted many features from our discussion here that one might include in an enhanced version of this model. Such enhancements may increase the applicability of the model in theoretical considerations involving SITR patterns occurring in loops of excitable media rather than in the context of human hearts. We can enhance the model by treating the UB functionally by refining the UB time window and considering bidirectional propagation in the loop, as noted above. Other enhancements to this model might include adding memory and latency to the APD restitution function. The inclusion of memory is especially important in clarifying the dynamic significance of delayed responses (not to mention improved fits to the APD restitution data). Additional directions for exploring the dynamics of the loop–pacer system include consideration of multiple exit/entry points into the loop that can affect reentry, consideration of multiple competing loops, and a systematic approach to heterogeneity.

References

Anastasiou-Nana, M.I., Menlove, R.L., Nanas, J.N., Anderson, J.L., 1988. Changes in spontaneous variability of ventricular ectopic activity as a function of time in patients with chronic arrhythmias. Circulation 78, 286–295.

Banville, I., Gray, R.A., 2002. Effects of action potential duration and conduction velocity restitution on alternans and the stability of arrhythmias. J. Cardiovas. Electrophysiol. 13, 1141–1149.

Bub, G., Tateno, K., Shrier, A., Glass, L., 2003. Spontaneous initiation and termination of complex rhythms in cardiac cell culture. J. Cardiovasc. Electrophysiol. 14, S229–S236.

Cain, J.W., 2007. Criterion for stable reentry in a ring of cardiac tissue. J. Math. Biol. 55, 433–448.

Cain, J.W., Schaeffer, D.G., 2006. Two-term asymptotic approximation of a cardiac restitution curve. SIAM Rev. 48, 537–546.

Cain, J.W., Tolkacheva, E.G., Schaeffer, D.G., Gauthier, D.J., 2004. Rate-dependent propagation of cardiac action potentials in a one-dimensional fiber. Phys. Rev. E 70, 061906.

Cao, J-M., Qu, Z., Kim, Y-H., Wu, T.-J., Garfinkel, A., Weiss, J.N., Karagueuzian, H.S., Chen, P-S., 1999. Spatiotemporal heterogeneity in the induction of ventricular fibrillation by rapid pacing: importance of cardiac restitution properties. Circ. Res. 84, 1318–1331.

Chay, T.R., Young, S.L., 1992. Studies on reentrant arrhythmias and ectopic beats in excitable tissues by bifurcation analysis. J. Theor. Biol. 155, 137–171.

Chen, X., Fenton, F.H., Gray, R.A., 2005. Head–tail interactions in numerical simulations of reentry in a ring of cardiac tissue. Heart Rhythm 2, 851–859.

Cheng, S.S., 2003. Partial Difference Equations. CRC Press, Boca Raton.

Cherry, E.M., Fenton, F.H., 2004. Suppression of alternans and conduction blocks despite steep APD restitution: electrotonic, memory, and conduction velocity restitution effects. Am. J. Physiol. 286, H2332–H2341.

Chialvo, D.R., Michaels, D.C., Jalife, J., 1990. Supernormal excitability as a mechanism of chaotic dynamics of activation in cardiac Purkinje fibers. Circ. Res. 66, 525–545.

Chow, A.W.C., Schilling, R.J., Davies, D.W., Peters, N.S., 2002. Characteristics of wave front propagation in reentrant circuits causing human ventricular tachycardia. Circulation 105, 2172–2178.

Courtemanche, M., Vinet, A., 2003. Reentry in excitable media. In: Beuter, A., Glass, L., Mackey, M.C., Titcombe, M.S. (Eds.), Nonlinear Dynamics in Physiology and Medicine. Springer, New York (Chapter 7).

Courtemanche, M., Glass, L., Keener, J.P., 1993. Instabilities of a propagating pulse in a ring of excitable media. Phys. Rev. Lett. 70, 2182–2185.

Courtemanche, M., Keener, J.P., Glass, L., 1996. A delay equation representation of pulse circulation on a ring in excitable media. SIAM J. Appl. Math. 56, 119–142.

Cytrynbaum, E., Keener, J.P., 2002. Stability conditions for the traveling pulse: modifying the restitution hypothesis. Chaos 12, 788–799.

De Bakker, J.M.T., Coronel, R., Tasseron, S., Wilde, A.A.M., Opthof, T., Janse, M.J., van Capelle, F.J.L., Becker, A.E., Jambroes, G., 1990. Ventricular tachycardia in the infarcted, Langendorff-perfused human heart: role of arrangement of surviving cardiac fibers. J. Am. Coll. Cardiol. 15, 1594–1607.

Derksen, R., van Rijen, H.V.M., Wilders, R., Tasseron, S., Hauer, R.N.W., Rutten, W.L.C., de Bakker, J.M.T., 2003. Tissue discontinuities affect conduction velocity restitution: a mechanism by which structural barriers may promote wave break. Circulation 108, 882–888.

Downar, E., Kimber, S., Harris, L., Mickleborough, L., Sevaptsidis, E., Masse, S., Chen, T.C., Genga, A., 1992. Endocardial mapping of ventricular tachycardia in the intact human heart. II. Evidence for multiuse reentry in a functional sheet of surviving myocardium. J. Am. Coll. Cardiol. 20, 869–878.

Elaydi, S.N., 1999. An Introduction to Difference Equations, second ed. Springer, New York.

Fox, J.J., Bodenschatz, E., Gilmour, R.F., 2002a. Period-doubling instability and memory in cardiac tissue. Phys. Rev. Lett. 89, 138101(04).

Fox, J.J., Gilmour, R.F., Bodenschatz, E., 2002b. Conduction block in one-dimensional heart fibers. Phys. Rev. Lett. 89, 198101(04).

Frame, L.H., Simson, M.B., 1988. Oscillations of conduction, action potential duration and refractoriness: a mechanism for spontaneous termination of reentrant tachycardias. Circulation 78, 2182–2185.

Gilmour, R.F., Watanabe, M.A., Otani, N.F., 1999. Restitution properties and dynamics of reentry. In: Cardiac Electrophysiology: From Cell to Bedside, Third ed. W.B. Saunders, London pp. 378–385.

Girouard, S.D., Pastore, J.M., Laurita, K.R., Gregory, K.W., Rosenbaum, D.S., 1996. Optical mapping in a new guinea pig model of ventricular tachycardia reveals mechanisms for multiple wavelengths in a single reentrant circuit. Circulation 93, 603–613.

Glass, L., Goldberger, A.L., Courtemanche, M., Shrier, A., 1987. Nonlinear dynamics, chaos and complex cardiac arrhythmias. Proc. R. Soc. London A 413, 9–26.

Hall, G.M., Bahar, S., Gauthier, D.J., 1999. Prevalence of rate-dependent behaviors in cardiac muscle. Phys. Rev. Lett. 82, 2995–2998.

Harris, L., Downar, E., Mickleborough, L., Shaikh, N., Parson, Chen, T., Gray, G., 1987. Activation sequence of ventricular tachycardia: endocardial and epicardial mapping studies in the human ventricle. J. Am. Coll. Cardiol. 10, 1040–1047.

Hwang, S.-M., Kim, T.Y., Lee, K.J., 2005. Complex-periodic spiral waves in confluent cardiac cell cultures induced by localized inhomogeneities. Proc. Natl. Acad. Sci. USA 102, 10363–10368.

Ito, H., Glass, L., 1992. Theory of reentrant excitation in a ring of cardiac tissue. Physica D 56, 84–106.

Jack, J.J., Noble, D., Tsien, R.W., 1975. Electric Current Flow in Excitable Cells. Clarendon Press, Oxford.

Jalife, J., Antzelevich, C., Moe, G.K., 1982. The case for modulated parasystole. Pace 5, 911–926.

Kalb, S.S., Dobrovolny, H.M., Tolkacheva, E.G., Idriss, S.F., Krassowska, W., Gauthier, D.J., 2004. The restitution portrait: a new method for investigating rate-dependent restitution. J. Cardiovasc. Electrophysiol. 15, 698–709.

Keener, J.P., 2002. Arrhythmias by dimension. In: Sneyd, J. (Ed.), An Introduction to Mathematical Modeling in Physiology, Cell Biology and Immunology. American Mathematical Society, Providence, RI, pp. 57–81.

Kocic, V.L., Ladas, G., 1993. Global Behavior of Nonlinear Difference Equations of Higher Order with Applications. Kluwer Academic Publishers, Dordrecht.

Koller, M.L., Riccio, M.L., Gilmour, R.F., 1998. Dynamic restitution of action potential duration during electrical alternans and ventricular fibrillation. Am. J. Physiol. 275, H1635–H1642.

Koller, M.L., Maier, S.K.G., Gelzer, A.R., Bauer, W.R., Meesman, M., Gilmour, R.F., 2005. Altered dynamics of action potential restitution and alternans in humans with structural heart disease. Circulation 112, 1542–1548.

Krebs, M.E., Szwed, J.M., Shinn, T., Miles, W.M., Zipes, D.P., 1998. Short-term rapid ventricular pacing prolongs ventricular refractoriness in patients. J. Cardiovasc. Electrophysiol. 9, 1036–1042.

Kunysz, A.M., Shrier, A., Glass, L., 1997. Bursting behavior during fixed-delay stimulation of spontaneously beating chick heart cell aggregates. Am. J. Physiol. 273, C331–C346.

Lampert, R., Rosenfeld, L., Batsford, W., Lee, F., McPherson, C., 1994. Circadian variation of sustained ventricular tachycardia in patients with coronary artery disease and implantable cardioverter defibrillators. Circulation 90, 241–247.

Liebovitch, L.S., Todorov, A.T., Zochowski, M., Scheurle, D., Colgin, L., Wood, M.A., Ellenbogen, K.A., Herre, J.M., Bernstein, R.C., 1999. Nonlinear properties of cardiac rhythm abnormalities. Phys. Rev. E 59, 3312–3319.

Lown, B., 1979. Sudden cardiac death: the major challenge confronting contemporary cardiology. Am. J. Cardiol. 43, 313–328.

Manios, E.G., Kallergis, E.M., Kanoupakis, E.M., Mavrakis, H.E., Mouloudi, H.K., Klapsinos, N.K., Vardas, P.E., 2005. Effects of successful cardioversion of persistent atrial fibrillation on right ventricular refractoriness and repolarization. Europace 7, 34–39.

Mickens, R., 1991. Difference Equations: Theory and Applications, second ed. CRC Press, Boca Raton.

Mines, G.R., 1913. On dynamic equilibrium in the heart. J. Physiol. (London) 46, 349–383.

Mitchell, C.C., Schaeffer, D.G., 2003. A two-current model for the dynamics of cardiac membrane. Bull. Math. Biol. 65, 767–793.

Moe, G.K., Jalife, J., Mueller, W.J., Moe, B., 1977. A mathematical model of parasystole and its application to clinical arrhythmias. Circulation 56, 968–979.

Nagai, Y., Gonzalez, H., Shrier, A., Glass, L., 2000. Paroxysmal starting and stopping of circulating waves in excitable media. Phys. Rev. Lett. 18, 184248(4).

Nolasco, J.B., Dahlen, R.W., 1968. A graphic method for the study of alternation in cardiac action potentials. J. Appl. Physiol. 25, 191–196.

Otani, N.F., Gilmour, R.F., 1997. Memory models for the electrical properties of local cardiac systems. J. Theor. Biol. 187, 409–436.

Plonsey, P., Barr, R.C., 2000. Bioelectricity: A Quantitative Approach, second ed. Kluwer Academic Press, Plenum Press, NY.

Qu, Z., Weiss, J.N., Garfinkel, A., 1997. Spatiotemporal chaos in a simulated ring of cardiac cells. Phys. Rev. Lett. 78, 1387–1390.

Quan, W., Rudy, Y., 1990. Unidirectional block and reentry of cardiac excitation: a model study. Circ. Res. 66, 367–382.

Sedaghat, H., 2003. Nonlinear Difference Equations: Theory with Applications to Social Science Models. Kluwer Academic Publishers, Dordrecht.

Sedaghat, H., Kent, C.M., Wood, M.A., 2005. Criteria for the convergence, oscillation and bistability of pulse circulation in a ring of excitable media. SIAM J. Appl. Math. 66, 573–590.

Stein, K.M., Borer, J.S., Hochreiter, C., Kligfield, P., 1992. Fractal clustering of ventricular ectopy and sudden death in mitral regurgitation. J. Electrocardiol. 25 (suppl), 178–181.

Stubna, M.D., Rand, R.H., Gilmour, R.F., 2002. Analysis of a nonlinear partial difference equation, and its application to cardiac dynamics. J. Difference Equations Appl. 8, 1147–1169.

Ten Tusscher, K.H.W.J., Bernus, O., Hren, R., Panfilov, A.V., 2006. Comparison of electrophysiological models for human ventricular cells and tissues. Prog. Biophys. Mol. Biol. 90, 326–345.

Vinet, A., 2000. Quasiperiodic circus movement in a loop model of cardiac tissue: multistability and low dimensional equivalence. Ann. Biomed. Eng. 28, 704–720.

Watanabe, M.A., Fenton, F.H., Evans, S.J., Hastings, H.M., Karma, A., 2001. Mechanisms for discordant alternans. J. Cardiovasc. Electrophysiol. 12, 196–206.

Watanabe, M.A., Koller, M.L., 2002. Mathematical analysis of dynamics of cardiac memory and accommodation: theory and experiment. Am. J. Physiol. 282, H1534–H1547.

Winkle, R.A., Derrington, D.C., Schroeder, J.S., 1977. Characteristics of ventricular tachycardia in ambulatory patients. Am. J. Cardiol. 39, 487–492.

Wood, M.A., Simpson, P.M., Stambler, B.S., Herre, J.M., Bernstein, R.C., Ellenbogen, K.A., 1995a. Long-term temporal patterns of ventricular tachyarrhythmias. Circulation 91, 2371–2377.

Wood, M.A., Simpson, P.M., London, W.B., Stambler, B.S., Herre, J.M., Bernstein, R.C., Ellenbogen, K.A., 1995b. Circadian patterns of ventricular tachycardia in patients with implantable cardioverter defibrillators. J. Am. Coll. Cardiol. 25, 901–907.

Wood, M.A., Simpson, P.M., Liebovitch, L.S., Todorov, A.T., Ellenbogen, K.A., 1997. Temporal patterns of ventricular tachyarrhythmias: insights from the implantable cardioverter-defibrillator. In: Dunbar, S.B., Ellenbogen, K.A., Epstein, A.E. (Eds.), Sudden Cardiac Death: Past, Present and Future. Futura Publishing Co, Armonk, NY.